A New Bi-Level Mathematical Model and Algorithm for VONs Mapping Problem

HEJUN XUAN [1], **SHIWEI WEI** [2], **YAN FENG** [1,3], **HUAPING GUO** [1,3], **AND YANLING LI** [1,3]

[1] School of Computer and Information Technology, Xinyang Normal University, Xinyang 464000, China
[2] School of Computer and Technology, Guilin University of Aerospace Technology, Guilin 541000, China
[3] Henan Key Laboratory of Analysis and Application of Education Big Data, Xinyang Normal University, Xinyang 464000, China

Corresponding author: Hejun Xuan (xuanhejun0896@126.com)

ABSTRACT Elastic optical networks (EONs) virtualization can allow the virtual optical networks (VONs) to utilize all the physical resources of EONs, and can attain a high performance of the networks. However, the optimal scheme for VONs mapping should be determined. To tackle these challenges, a bi-level mathematical model is established. leader's and follower's objectives are to minimize energy consumption and the maximum index of used frequency slots, respectively. The bi-level mathematical model can determine the optimal schemes of VONs mapping. To solve the mathematical model effectively, a uniform design method is applied to generate initial population for the lower level problem. In addition, To solve the whole model effectively, a tailor-made encoding, population initialization, genetic operators and local search operator are designed. An efficient genetic algorithm with local search operator is proposed for the bi-level mathematical model. To evaluate the mathematical model and the designed algorithm, a large number of experiments are performed on three kinds of the widely used networks, and the experimental results indicate that the effectiveness of the proposed bi-level mathematical model and designed algorithms.

INDEX TERMS Bi-level optimization, VONs mapping, spectrum assignment, VONs, local search.

I. INTRODUCTION

The booming of internet based activities requires an high performance internet network [3], [41]. Wavelength division multiplexing (WDM) networks cannot provide these requirements adaptively, they are low efficient [2], [15]. The recent elastic optical networks (EONs) can provide the these requirements adaptively to each request and get higher performance by using the orthogonal frequency division multiplexing (OFDM) [8], [13]. In addition, network virtualization can help to increase the flexibility of the network and can accelerate innovation of network architectures. Network virtualization technology not only allows the rock-bottom resource to be abstracted by applications, but also can be applied to the EONs and enables virtual optical networks (VONs) providers

to customize their infrastructure to different requirements of the client service [29], [49].

The virtualization of EONs has many superiorities and can promote VONs with various topologies. Furthermore, it can make the VONs to share the resources of the physical networks among the different users and applications, reduces physical resource management, offer simple spectrum assignment [6], [19], [32]. However, a challenge is how to map a large number of VONs with different topologies to the physical network while reaching some purpose, such as energy consumption, ratio of blocking, performance of the network [30]. In recent years, there are large number of researches focusing their research on the VONs mapping problem and some related problems [23], [42].

VONs mapping problem and spectrum assignment problem, where virtual connection requests are known in advance or are referred to as semi-dynamic users services, is investigated. Similar to other works, there is a assumption

---

The associate editor coordinating the review of this manuscript and approving it for publication was Tianhua Xu [ID].

that the system resource is sufficient. In other words, the blocking ratio of the virtual connection requests is zero. However, existed works that did not consider the hierarchical relation of the network systems and only required one objective to be optimal. In stead, we consider the hierarchical relation of the network systems and require two objectives to be optimal simultaneously, i.e., our two objectives are to minimize the energy consumption (EC) and the maximum index of used frequency slots (MIUFS) at the same time. Since the two objectives belong to two level decision makers, these two level decision makers have a hierarchical relationship. Thus, we can establish a bi-level mathematical model with minimizing the EC and the MIUFS as the leader's objective and follower's objective, respectively. For the bi-level optimization model, leader's decision and follower's decision are affected each other, and leader makes his/her decision first by determining the virtual nodes mapping scheme with the objective to minimize the EC, and then the follower makes the reaction by determining the virtual links mapping that implements routing and spectrum assignment scheme with the objective to minimize the MIUFS.

To solve the bi-level optimization model, we propose a genetic algorithm that is specifically designed with two populations is proposed. The major contributions of this study are summarized as follows:

- Different from the existing works, we require both the energy consumption (EC) and the maximum index of used frequency slots (MIUFS) to be minimized when the VON mapping and spectrum assignment problem is handled. Thus, the model has two objectives that includes leader's and follower's objectives.
- We consider the hierarchical relationship of the network systems. Thus, the two objectives have different priorities, and we establish a bi-level mathematical model with minimizing the EC of the EON as the leader's objective and minimizing the MIUFS as the follower's objectives.
- To solve the bi-level mathematical model effectively, tailor-made encoding, population initialization, genetic operators and local search operator are designed. An efficient genetic algorithm with local search operator is proposed for the bi-level mathematical model.

The rest of the paper is organized as follows. The related works are introduced in Section II. Section III describes the problem and establishes a novel bi-level mathematical model. To solve the established mathematical model with high performance, we propose a genetic algorithm with powerful local search and well-designed genetic operators in section IV. Section V presents experimental results and analysis. Conclusions with a summary are drawn in Section VI.

II. RELATED WORKS
A. VONs MAPPING PROBLEM
In order to address the VON mapping problem, a mixed integer mathematical model is established [40], and a traffic-matrix-based scheduling scheme is proposed to get the

optimal schemes. In cloud computing environments, the role of dynamic VON mapping problem is addressed [33]. An effective VON mapping algorithm is presented to provide efficient virtual infrastructures services to satisfy various users' requirements. To address the VON mapping problem, an integer linear mathematical model is set up, and an efficient scheme based on layered-auxiliary-graph (LAG) is presented in [18]. The cost of EONs and conventional wavelength division multiplexing networks is compared [39]. In addition, this paper also gives an outlook of the cost benefits for the operation of future optical transport networks. In order to minimize network cost in the multi-layer EONs, Two integer linear mathematical models are formulated, and a efficient algorithm, which based on greedy heuristic and tabu-search heuristic approach, is designed [11]. For the sake of minimizing EC and increasing spectrum usage [5], EC and spectrum usage aware VONs mapping methods are presented by using the minimum-sub-matrix scheme. Also, there are some other similar researches on the VON mapping problem [7], [35], [46]. However, almost all existing works formulated the VON mapping problem as a single level integer linear mathematical model or a single level mixed integer mathematical model, and did not consider the hierarchical relation of the network system in the model, and thus these models could not fit the real situation of the networks very well.

B. BI-LEVEL MATHEMATICAL PROBLEM AND GENETIC ALGORITHM
To solve the context of unbalanced economic markets problem, Stackelberg and Peacock [36] introduced the bi-level mathematical problem (BLPP), which can be viewed as a static version of the non-cooperative and two-person-game [1]. Bi-level mathematical is a technique which can be used to modeling decentralized decision problem. It consists of the leader-level and follower-level objectives [26]. If x and y denote the leader's decision variables and follower's decision variables, generic bi-level mathematical problem can be written as

$$\min_{x} U(x, y)$$

where y is obtained by solving the follower level optimization problem

$$\min_{y} L(x, y)$$

In this mathematical model, the evaluation of the leader-level objective function requires solving the follower-level problem. That is to say, leader decision maker cannot minimize its objective without the reactions of the followers considered. In general, bi-level optimization model is a NP-hard problem [16], [51]. In addition, bi-level optimization model has a leader objective, a follower objective and constrained conditions. Thus, bi-level optimization model is an optimization problem [28], [47]. There are numerous of algorithms focusing on solving bi-level mathematical problem, like methods based on vertex enumeration and meta-heuristics [17], [25].
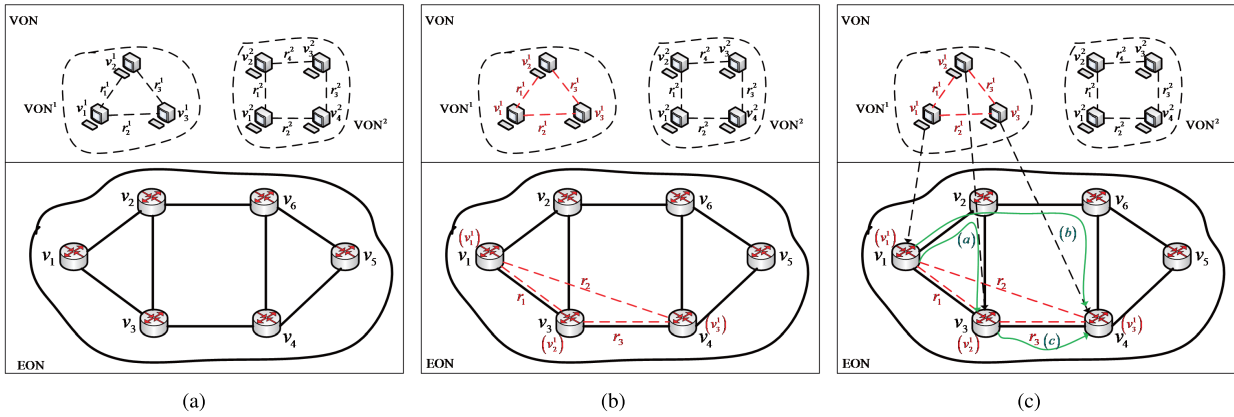
FIGURE 1. VONs mapping. (a) Physical network and VONs; (b) virtual nodes mapping; (c) virtual links mapping.

Genetic algorithms invented by Holland [20], have been proven to be an effective technique for many hard problems such as production-distribution planning problems [21], transportation and network design [45], Scientific workflow scheduling [43], task scheduling in cloud computing [34], [44], topology or size optimization [24]. However, it is not suitable to directly apply the aforementioned algorithms to the problems of VONs mapping in EONs, and it is necessary to make some improvements or revisions on them.

III. PROBLEM DESCRIPTION AND BI-LEVEL MATHEMATICAL MODEL FORMULATION

A. PHYSICAL ELASTIC OPTICAL NETWORKS

We use an undirected graph $G = (V, E)$ to denote an EONs. $V = \{v_1, v_2, \cdots, v_{N_V}\}$ is the set of the optical nodes in the network, and N_V is the number of nodes. v_i the i-th optical node. $E = (l_{ij})_{N_V \times N_V}$ is a matrix of optical links. $l_{ij} = 1$ if and only if there is an optical link between v_i and v_j. In general, $l_{ij} = l_{ji}$. N_E is the number of links in the network. In our work, we assume that there are $c(v_i)$ virtual machines (VMs) in node v_i. $F = \{f_1, f_2, \cdots, f_{N_F}\}$ represents the set of available frequency slots (FSs) in each optical link, where N_F denotes the number of available FSs. Like the existing works [13], [48], each FS has the same bandwidth C_{fs}. Therefore, the capacity of each FS is $ML \times C_{fs}$, where ML is the bits per symbol in a given modulation format. ML can be assigned as 1, 2, 3, 4, 5 and 6 for different modulation format of BPSK, QPSK, 8QAM, 16QAM, 32QAM and 64QAM.

B. VIRTUAL OPTICAL NETWORKS

$VON = \{VON^1, VON^2, \cdots, VON^M\}$ denotes a series of VONs on an EONs, where M is the number of VONs. $V^m = \{v_1^m, v_2^m, \cdots, v_{N_m}^m\}$ denotes the set of virtual nodes in m-th VON VON^m, where N_m is the number of virtual nodes in VON^m. Generally speaking, we have $N_m \leq N$. Let $N' = \sum_{m=1}^{M} N_m$ denote the number of virtual nodes in all VONs. Each virtual node $v_n^m(v_n^m \in V^m)$ has a series of candidate physical nodes Ω_n^m, and the physical nodes in Ω_n^m are all adjacent. That is to say, v_n^m can only be mapped to the

nodes in Ω_n^m. If a virtual node is mapped to a physical node $v_i(v_i \in V)$, one virtual machine on v_i will be occupied. So, the number of virtual nodes mapped to physical node v_i must be less than $c(v_i)$. Let $R^m = \{r_1^m, r_2^m, \cdots, r_{N_{R^m}}^m\}$ denote a set of virtual connection requests in VON^m, where N_{R^m} is the number of virtual connection requests in VON^m. So there are $N_R = \sum_{m=1}^{M} N_{R^m}$ virtual connection requests. $r_k^m(r_k^m \in R^m)$ is the k-th virtual connection request in VON^m which can be described as $r_k^m = (s_k^m, d_k^m, T_k^m)$, where $s_k^m(s_k^m, d_k^m \in V^m)$ is virtual source node, $d_k^m(s_k^m, d_k^m \in V^m)$ is virtual destination node. T_k^m is the capacity of r_k^m required.

C. VIRTUAL OPTICAL NETWORK MAPPING

First, we should determine the virtual nodes mapping scheme, i.e., virtual source nodes and destination node should be mapped to two different nodes in EONs. For $r_k^m = (s_k^m, d_k^m, T_k^m)$, if virtual nodes s_k^m and d_k^m are mapped to physical nodes $s_{k'}$ and $d_{k'}(s_{k'}, d_{k'} \in V)$, r_k^m will be translated to a physical connection request $r_{k'} = (s_{k'}, d_{k'}, T_{k'})$, where $T_{k'} = T_k^m$. When all virtual nodes are mapped to the nodes in EONs, all the virtual connection requests can be translated to connection requests(we use connection requests to denote physical connection requests through this paper). $R' = \{r_1, r_2, \cdots, r_{N_{R'}}\}$ and $N_{R'}$ denote a series of connection requests and the number of connection requests, respectively. Since a virtual connection request is corresponding to a connection request, therefore, we have $N_{R'} = N_R$. As shown in Fig.1a, there are two VONs on the physical optical network. In virtual optical network VON^1, there are three virtual nodes. Virtual link (dashed line) exists between each pair of virtual nodes and denotes a virtual connection request. The set of candidate physical nodes of all virtual nodes in VON^1 are v_1, v_2, v_3, v_4. As shown in Fig.1b, virtual nodes v_1^1, v_2^1 and v_3^1 are mapped to physical nodes v_1, v_3 and v_4, virtual connection requests $r_1^1 = (v_1^1, v_2^1, T_1^1)$, $r_2^1 = (v_1^1, v_3^1, T_2^1)$ and $r_3^1 = (v_2^1, v_3^1, T_3^1)$ are translated to connection requests $r_1 = (v_1, v_3, T_1)$, $r_2 = (v_1, v_4, T_2)$ and $r_3 = (v_3, v_4, T_3)$, respectively, and we have $T_i^1 = T_i(i = 1, 2, 3)$.

To handle connection requests, we should make the routing (routing is used for connection requests to instead of link mapping) for the connection requests in the EONs. As shown in Fig.1c, we choose paths (*a*), (*b*) and (*c*) (solid line in green) for connection request r_1, r_2 and r_3, respectively. So, virtual links $l_{v_1^1, v_2^1}$, $l_{v_1^1, v_3^1}$ and $l_{v_2^1, v_3^1}$ are mapped to physical paths (*a*), (*b*) and (*c*).

D. SPECTRUM ASSIGNMENTS

Each link has a series of FSs, and a connection request occupies one or much more FSs. The procedure, which is to assigning several FSs to a connection request, is called spectrum assignment. When we assign spectra for all connection requests, three constraints should be satisfied: (1) Spectrum consistency means that the start index of FSs on different links of a path must be uniform; As shown in Fig.2, there are eight FSs on each link, and the indexes are from 1 to 8 (Only are the frequency slots on l_{12} and l_{26} drawn in Fig. 2). Assuming that there is a connect request $r_{k'}$, and l_{12} and l_{26} are two links in the path of $r_{k'}$ occupied. If the frequency slot 2, 3 and 4 on link l_{12} are assigned to $r_{k'}$, the frequency slot 2, 3 and 4 on link l_{26} must be assigned to $r_{k'}$. (2) Several consecutive FSs must be assigned to a connection request. We can assign the frequency slot 2, 3 and 4 on link l_{12} to $r_{k'}$. However, we cannot assign the frequency slot 2, 3 and 5 on link l_{12} to $r_{k'}$. (3) One FSs on a link only can be assigned to one connection request. Two connect request $r_{k'}$ and $r_{k''}$ are occupied the same link l_{12}. If we assign the frequency slot 3 on link l_{12} to $r_{k'}$, we cannot assign the frequency slot 3 on link l_{12} to $r_{k''}$.
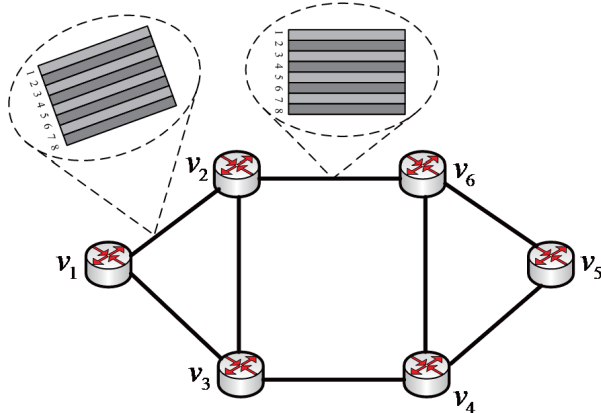

FIGURE 2. Spectrum and spectrum assignment.

E. BI-LEVEL MATHEMATICAL MODEL FOR VONs MAPPING

The challenge problem of virtual nodes mapping, routing and spectrum assignment in EONs can be summarized as: virtual nodes in all VONs must be mapped to nodes in EONs. Then, optimal paths should be selected for all the connection requests in EONs, i.e., virtual link mapping (routing). Finally, spectrum assignment scheme should be determined for all the connection requests. In addition, virtual nodes mapping scheme and routing scheme have an effect on the EC, and routing scheme and spectrum assignment scheme can affect the MIUFS. So, virtual nodes mapping scheme and routing scheme should be determined to minimize EC. To minimize the maximum index of used frequency slots, optimal routing scheme and spectrum assignment scheme will be determined based on the predetermined virtual nodes mapping scheme. Considering the hierarchical features of the problem, we establish a bi-level mathematical model with minimizing the EC of the EONs as the leader's objective and minimizing the MIUFS as the follower's objectives, respectively. To minimize EC, leader level decision maker will determine the virtual nodes mapping scheme and routing scheme for all the virtual connection requests. Then, to minimize the MIUFS, follower level decision maker will make the reaction to determine the optimal routing scheme and spectrum assignment scheme based on the virtual nodes mapping scheme that leader level decision maker has determined.

1) LEADER's OBJECTIVE

In the bi-level mathematical model, the objective of leader decision maker is to minimize the EC for all the connection requests by determining virtual nodes mapping scheme and routing scheme. So, the objective function of the leader can be given by

$$\min E_{total} = \min \left\{ \sum_{k'=1}^{N_{R'}} \left(\lambda_{k'}^q g(Q_{k'}^q) \right) \right\} \quad (1)$$

where $Q_{k'}^q$ is q-th path in the set $Q_{k'}$ of candidate paths of connection request $r_{k'}$. $g(Q_{k'}^q)$ is energy consumption when connection request $r_{k'}$ occupies the path $Q_{k'}^q$. $\lambda_{k'}^q$ is a boolean variable, $\lambda_{k'}^q = 1$ when the path $Q_{k'}^q$ is occupied by $r_{k'}$, otherwise, $\lambda_{k'}^q = 0$. $g(Q_{k'}^q)$ is the EC of $r_{k'}$ on path $Q_{k'}^q$ and is calculated by the method in [37].

The number of required frequency slots $B_{k'}$ and modulation format $ML_{k'}$ of $r_{k'}$ selected on path $Q_{k'}^q$ should be determined. Since each FS has the same bandwidth C_{fs}. Therefore, the capacity of an FS is $ML_{k'} \times C_{fs}$, the number of FSs of $r_{k'}$ required $B_{k'}$ is calculated by

$$B_{k'} = \left\lceil \frac{T_{k'}}{ML_{k'} \times C_{fs}} \right\rceil, \quad (2)$$

and $ML_{k'}$ is determined by

$$ML_{k'} = \max \left\{ ML | L(ML) \geq \sum_{l_{ij} \in Q_{k'}^q} d(l_{ij}) \right\}, \quad (3)$$

where $d(l_{ij})$ is the length of link l_{ij}.

The leader's decision must be made under some constraint conditions as follows:

Constraint (a): one node in VONs should be mapped to one its candidate node in EONs. We can express this constraint by

$$\sum_{v_i \in \Omega_n^m} \theta_{n,i}^m \times \left(1 - \sum_{v_i \in V \setminus \Omega_n^m} \theta_{n,i}^m \right) = 1, \quad \forall v_n^m \in V \quad (4)$$

where $\theta_{n,i}^m$ is a boolean variable. $\theta_{n,i}^m = 1$ when v_n^m is mapped to node v_i, otherwise, $\theta_{n,i}^m = 0$.

Constraint (b): Two different virtual nodes in one VONs should not be mapped to the identical node in EONs. For v_n^m in VON^m, we have

$$\sum_{n=1}^{N_m} \theta_{n,i}^m \leq 1, \quad \forall VON^m \in VON \tag{5}$$

Constraint (c): The number of nodes mapped to physical node must be less than the number of virtual machine on the node in EONs. For node $v_i(\forall v_i \in V)$, this constraint can be expressed by

$$\sum_{m=1}^{M} \sum_{n=1}^{N_m} \theta_{n,i}^m \leq c(v_i), \quad \forall v_i \in V \tag{6}$$

2) FOLLOWER's OBJECTIVE
The follower's objective is to minimize the MIUFS by looking for the optimal schemes of routing and spectrum assignment for all the connection requests. So, the follower's objective function can be written by

$$\min N(F) = \min \left\{ \max_{l_{ij} \in E} \left\{ N(F_{l_{ij}}) \right\} \right\} \tag{7}$$

where $N(F_{l_{ij}})$ is the MIUFS on link l_{ij}.

Similar to the leader' decision, follower decision also must be under some constraints conditions:

Constraint (d): For $r_{k'}(\forall r_{k'} \in R')$, it only can occupy one path. That is,

$$\sum_{q=1}^{N_{Q_{k'}}} \lambda_{k'}^q = 1, \quad \forall r_{k'} \in R' \tag{8}$$

Constraint (e): For $r_{k'}(\forall r_{k'} \in R')$, the start index of occupied FSs on different links of one path should be identical. It can be given by

$$f_{l_{ij}}^{k'} = f_{l_{i'j'}}^{k'}, \quad \forall r_{k'} \in R' \tag{9}$$

where $f_{l_{ij}}^{k'}$ and $f_{l_{i'j'}}^{k'}$ are the start index of occupied FSs of $r_{k'}$ on links l_{ij} and $l_{i'j'}$, respectively, and l_{ij} and $l_{i'j'}$ are two different links in $r_{k'}$ occupied path.

Constraint (f): Several consecutive FSs must be assigned to a connection request $r_{k'}(\forall r_{k'} \in R')$. We can express this constraint by

$$\sum_{u=f_{l_{ij}}^{k'}}^{f_{l_{ij}}^{k'}+B_{k'}+GF-1} \phi_{k',l_{ij}}^{q,u} = B_{k'} + GF, \quad \forall r_{k'} \in R' \tag{10}$$

where $\phi_{k',l_{ij}}^{q,u}$ is a boolean variable. $\phi_{k',l_{ij}}^{q,u} = 1$ when the u-th FS on link l_{ij} of path $Q_{k'}^q$ is occupied by connection request $r_{k'}$, otherwise, $\phi_{k',l_{ij}}^{q,u} = 0$. GF is the number of guaranteed frequency slots.

Constraint (g): For any two different $r_{k'}$ and $r_{k''}$ which has the same link l_{ij} in their occupied path, if the start index

frequency slot of $r_{k'}$ occupied is smaller than that of $r_{k''}$, this case is denoted by $r_{k'} \prec r_{k''}$. Then $r_{k'}$ and $r_{k''}$ should satisfy

$$f_{l_{ij}}^{k'} + B_{k'} + GF - 1 \leq f_{l_{ij}}^{k''}, \quad \forall r_{k'} \prec r_{k''} \tag{11}$$

This in-equation means that the index of the last frequency slot of connection requests $r_{k'}$ occupied should be not greater than the index of the first frequency slot of connection requests $r_{k''}$.

Based on leader's and follower's objectives and constraints, a bi-level mathematical model is estimated as follows:

$$\begin{cases} \min E_{total} = \min \left\{ \sum_{k'=1}^{N_{R'}} \left(\lambda_{k'}^q g(Q_{k'}^q) \right) \right\} \\ s.t. \\ (a) \sum_{v_i \in \Omega_n^m} \theta_{n,i}^m \times \left(1 - \sum_{v_i \in V \setminus \Omega_n^m} \theta_{n,i}^m \right) = 1; \\ (b) \sum_{n=1}^{N_m} \theta_{n,i}^m \leq 1; \\ (c) \sum_{m=1}^{M} \sum_{n=1}^{N_m} \theta_{n,i}^m \leq c(v_i); \\ \min N(F) = \min \left\{ \max_{l_{ij} \in E} \left\{ N(F_{l_{ij}}) \right\} \right\} \\ s.t. \\ (d) \sum_{q=1}^{N_{Q_{k'}}} \lambda_{k'}^q = 1; \\ (e) f_{l_{ij}}^{k'} = f_{l_{i'j'}}^{k'}; \\ (f) \sum_{u=f_{l_{ij}}^{k'}}^{f_{l_{ij}}^{k'}+B_{k'}+GF-1} \phi_{k',l_{ij}}^{q,u} = B_{k'} + GF; \\ (g) f_{l_{ij}}^{k'} + B_{k'} + GF - 1 \leq f_{l_{ij}}^{k''}; \end{cases} \tag{12}$$

To solve this bi-level mathematical model, we propose an effective genetic algorithm using uniform design in section IV.

IV. PROPOSED GENETIC ALGORITHM
The proposed model above is a bi-level optimization problem and is a NP-hard optimization problem. Usual algorithms cannot solve this problem efficiently [9], [14], [46]. To solve the proposed bi-level mathematical model effectively, we propose an improved genetic algorithm and denote it as GAL. In the following subsection, we will give the genetic operators designed in detail.

A. ENCODING AND DECODING
1) ENCODING
To solve the virtual optical network mapping and spectrum assignment problem, four necessary steps are needed: 1) virtual nodes in VONs should be mapped to physical

nodes in EONs; 2) connection requests are sorted by using some specific strategy; 3) routing; 4) spectrum assignment. In this work, the connection requests are sorted randomly and do not need to encode. In addition, first fit is used to spectrum assignment [22]. Therefore, it is not need to encode for sorting and spectrum assignment. Thus, it only has two populations, i.e., virtual nodes mapping population and routing population.

In virtual nodes mapping population, each individual presents a virtual nodes mapping scheme. We assume that $x = (x_1, x_2, \cdots, x_{n'}, \cdots, x_{N'})$ is an individual in virtual nodes mapping population. For example, there are six nodes and eight links in the physical EONs and two VONs (VON_1 and VON_2) on the EONs. VON_1 has three virtual nodes (v_1^1, v_2^1 and v_3^1) and three virtual links, and VON_2 has four virtual nodes (v_1^2, v_2^2, v_3^2 and v_4^2) and four virtual links. If v_1^1, v_2^1, v_3^1 are mapped to v_1, v_3, v_4, and $v_1^2, v_2^2, v_3^2, v_4^2$ are mapped to v_2, v_4, v_5, v_6, we can encode this scheme as $(1, 3, 4, 2, 4, 5, 6)$.

Similar to virtual nodes mapping population, in the routing population, each routing individual presents a scheme of routing for all the connection requests. Assuming that $y = (y_1, y_2, \cdots, y_{k'}, \cdots, y_{N_{R'}})$ is an routing individual. $y_{k'} = q$ when $r_{k'}$ occupies q-th path in candidate paths set $Q_{k'}$ of connection request $r_{k'}$, i.e., $\lambda_{k'}^q = 1$. Assuming that $r_1^1, r_2^1, r_3^1, r_4^1$ select the 2-th, 1-th, 5-th, 4-th in there candidate paths set, and $r_1^2, r_2^2, r_3^2, r_4^2$ select the 1-th, 2-th, 4-th, 3-th in there candidate path set. According to the encoding scheme, we can encode this scheme as $(2, 1, 5, 4, 1, 2, 4, 3)$.

2) DECODING

For a given virtual nodes mapping individual $x = (x_1, x_2, \cdots, x_{n'}, \cdots, x_{N'})$. If $x_{n'} = i$, v_n^m in VON^m is mapped to v_i, where m and n are calculated by

$$m = \min \left\{ \left\{ m \mid \sum_{m'=1}^{m} N_{m'} \geq n', m \leq M \right\} \right\} \quad (13)$$

$$n = n' - \sum_{m'=1}^{m-1} N_{m'} \quad (14)$$

Similarly, $y = (y_1, y_2, \cdots, y_{k'}, \cdots, y_{N_{R'}})$ is a routing individual. If $y_{k'} = q$, $r_{k'}$ occupies the q-th path in its candidate path set $Q_{k'}$, i.e., $Q_{k'}^q$.

3) POPULATION INITIALIZATION

In proposed algorithm, two populations, virtual nodes mapping and routing populations, are needed. Virtual nodes mapping population can be generated by Algorithm 1. In routing population initiation algorithm, uniform design [27], [38] is used to generate the routing individuals. The two Algorithms have an advantage that the individuals in initialized virtual nodes mapping population and routing population are all the feasible solutions. To understand Algorithm of routing population initiation clearly, we first introduce the uniform design method.

Algorithm 1 Virtual Nodes Mapping Population Initialization

Input: Candidate set Ω_n^m, Population size Pop_{size}
Output: Mapping population MP

1: **for** $p = 1$ to Pop_{Size} **do**
2:     $flag1\_succ = 0$;
3:     **while** $flag1\_succ == 0$ **do**
4:       **for** $m = 1$ to M **do**
5:         **for** $n = 1$ to N_m **do**
6:           $t\Omega_n^m = \Omega_n^m$; $n' = \sum_{m'=1}^{m-1} N_{m'} + n$; $flag2\_succ = 0$;
7:           **while** $flag2\_succ == 0$ **do**
8:             **if** $N_{t\Omega_n^m} > 0$ **then**
9:               % $N_{t\Omega_n^m}$ is the number of nodes in $t\Omega_n^m$;
10:               An integer i' is generated randomly between 1 and $N_{t\Omega_n^m}$;
11:               num is the number of $t\Omega_n^m(i')$ appeared in $MP(p, 1 : n')$;
12:               **if** $num \leq c(v_{t\Omega_n^m(i')})$ **then**
13:                 $flag2\_succ = 1$;
14:                 $MP(p, n') = t\Omega_n^m(i')$;
15:               **else**
16:                 $flag2\_succ = 0$;
17:               **end if**
18:             **else**
19:               $flag2\_succ = 0$;
20:               $t\Omega_n^m = t\Omega_n^m \setminus \{t\Omega_n^m(i')\}$;
21:             **end if**
22:           **end while**
23:         **end for**
24:         **if** $flag2\_succ == 0$ **then**
25:           break;
26:         **end if**
27:       **end for**
28:       **if** $flag2\_succ == 0$ **then**
29:         break;
30:       **else**
31:         **if** $m == M$ **then**
32:           $flag1\_succ = 1$;
33:         **end if**
34:       **end if**
35:     **end while**
36: **end for**

Overview of Uniform Design: To generate points to be uniformly distributed on the experimental domain, uniform design method was developed [27], [38]. It generates a small number of the uniformly distributed representative points in a domain by using a uniform array $U(S, H) = [U_{i,j}]_{H \times S}$, where $U_{i,j}$ denotes the level of the j-th factor in the i-th combination with the j-th factor representing the j-th variable and its level being its value [21].

To construct uniform design array, many methods are presented [27]. Not only simple but also efficient method proposed in [27]. Firstly, we construct a hypercube over an S-dimensional space:

$$C^S = \{(c_1, c_2, \cdots, c_S) | a_i \le c_i \le b_i, i = 1, 2, \cdots, S\}$$

where a_i and b_i are the lower and upper bounds of the i-th factor (i.e., i-th variable), respectively. Then, a hyper-rectangle is formed between a_i and d_i as follows:

$$C(d) = \{(c_1, c_2, \cdots, c_S) | a_i \le c_i \le d_i, i = 1, 2, \cdots, S\} \subset C^S$$

Finally, H uniformly distributed points are selected randomly from C^S. Assuming that $H(d)$ is the number of points fallen into the hyper-rectangle $C(d)$, and the fraction of points in $C(d)$ is $H(d)/H$. As the volume of hypercube C^S is $\prod_{i=1}^S (b_i - a_i)$, so the volume of $C(d)$ is $\prod_{i=1}^S (d_i - a_i)$. The H uniform distributed points in C^S should minimize

$$\sup_{x \in C^S} \left\{ \frac{H(d)}{H} - \frac{\prod_{i=1}^S (d_i - a_i)}{\prod_{i=1}^S (b_i - a_i)} \right\} \quad (15)$$

Hence, we can map these H points in C^S to the problem domain with S factors and χ levels uniformly, where H is an odd and $H > S$. It has been proved that $U_{i,j}$ can be given by [27]:

$$U_{i,j} = (i\sigma^{j-1} \mod \chi) + 1 \quad (16)$$

where σ is a constant related to the number of factors S and level χ. The H sample points scattered uniformly in the hypercube can be selected.

B. CROSSOVER OPERATORS

Since two different populations exist in the proposed model, different crossover operators are presented. Crossover operator to generate new virtual nodes mapping individual is presented in Algorithm 2. To generate new routing individuals, crossover operator is described in detail as follows: two routing individuals y^1 and y^2 are selected randomly as the parents from the current population. Let $L_p = (A_1, A_2, \cdots, A_{N_{R'}})$ and $U_p = (B_1, B_2, \cdots, B_{N_{R'}})$ be defined by:

$$\begin{cases} L_p = \left[\min(y_1^1, y_1^2), \min(y_2^1, y_2^2), \cdots, \min(y_{N_{R'}}^1, y_{N_{R'}}^2) \right] \\ U_p = \left[\max(y_1^1, y_1^2), \max(y_2^1, y_2^2), \cdots, \max(y_{N_{R'}}^1, y_{N_{R'}}^2) \right] \end{cases} \quad (17)$$

where $A_i = \min(y_i^1, y_i^2)$, $B_i = \max(y_i^1, y_i^2)$ ($i = 1, 2, \cdots, N_{R'}$). So, two routing offspring $y^{c1} = (y_1^{c1}, y_2^{c1}, \cdots, y_{N_{R'}}^{c1})$ and $y^{c2} = (y_1^{c2}, y_2^{c2}, \cdots, y_{N_{R'}}^{c2})$ are generated by

$$y_i^{c1} = \min \left\{ B_i, \left\lceil \frac{2A_i + B_i}{3} \right\rceil \right\} \quad (18)$$

$$y_i^{c2} = \max \left\{ A_i, \left\lfloor \frac{A_i + 2B_i}{3} \right\rfloor \right\} \quad (19)$$

Algorithm 2 Crossover Operator for Nodes Mapping Individual

Input: Mapping individual x, probability of crossover p_c, probability of neighbors selection p_n

Output: Offspring x^c obtained by crossover operator

1: **if** $rand() \le p_n$ **then**
2: An individual $x^1 = (x_1^1, x_2^1, \cdots, x_{N'}^1)$ is selected in the neighbors $neiber(x)$ of individual x;
3: **else**
4: An individual $x^1 = (x_1^1, x_2^1, \cdots, x_{N'}^1)$ is selected in the population except for the $neiber(x)$;
5: **end if**
6: $x^c = x$;
7: **for** $n' = 1$ to N' **do**
8: **if** $rand() \le p_c$ **then**
9:   num is the number of node $x_{n'}^1$ appeared in x;
10:   **if** $num + 1 > c(v_{x_{n'}^1})$ **then**
11:    m, n are calculated by formula (13) and formula (14).
12:    $t\Omega_n^m = \Omega_n^m \setminus \{x_{n'}^1, x_{n'}\}$;
13:    $flag = 0$;
14:    **while** $N_{t\Omega_n^m} > 0$ & $flag == 0$ **do**
15:     An integer i' is generated randomly between 1 and $N_{t\Omega_n^m}$;
16:     num is the number of $t\Omega_n^m(i')$ appeared in x^c;
17:     **if** $num + 1 > c(v_{t\Omega_n^m(i')})$ **then**
18:      $t\Omega_n^m = \Omega_n^m \setminus \{t\Omega_n^m(i')\}$;
19:      $flag = 0$;
20:     **else**
21:      $flag = 1$;
22:     **end if**
23:    **end while**
24:    **if** $flag == 1$ **then**
25:     $x_{n'}^c = t\Omega_n^m(i')$;
26:    **end if**
27:   **else**
28:    $x_{n'}^c = x_{n'}^1$;
29:   **end if**
30: **end if**
31: **end for**

We can see that the offspring of virtual nodes mapping individual and routing individual obtained by these two crossover operators are all the feasible solutions.

C. MUTATION OPERATORS

Similar to crossover operator, there are two different mutation operators for virtual nodes mapping individual and routing individual, respectively. The opposite-based search strategy is used to generate the new individuals of the routing population. For the virtual nodes mapping individual, we design a new mutation operator and present it in Algorithm 3. In Algorithm 3, step 5 and step 6 are using to generate

---

Algorithm 3 Mutation Operator for Nodes Mapping Individual

Input: Mapping individual x^c, probability of mutation p_m;

Output: Offspring x^m obtained by mutation operator

1: $x^m = x^c$
2: $flag = 0, count = 0$;
3: **while** $(flag == 0) \& (count <= N'/2)$ **do**
4:    $count = count + 1$;
5:    Two integers $m, n (1 \leq m \leq M, 1 \leq n \leq N_m)$ are generated randomly;
6:    $n' = \sum\limits_{m'=1}^{m} N_{m'} + n$;
7:    $t\Omega_n^m = \Omega_n^m \setminus \{x_{n'}\}$;
8:    **while** $N_{t\Omega_n^m} > 0$ **do**
9:       An integer i' is generated randomly between 1 and $N_{t\Omega_n^m}$;
10:       num is the number of $t\Omega_n^m(i')$ appeared in x^m;
11:       **if** $num + 1 < c(v_{t\Omega_n^m(i')})$ **then**
12:          $x_{n'}^m = t\Omega_n^m(i')$;
13:          $flag = 1$;
14:       **else**
15:          $t\Omega_n^m = t\Omega_n^m \setminus \{t\Omega_n^m(i')\}$;
16:       **end if**
17:    **end while**
18: **end while**

Algorithm 4 Local Search Operator for Routing Individual

Input: Individual $y = (y_1, y_2, \cdots, y_{N_{R'}})$;

Output: New individual $y' = (y'_1, y'_2, \cdots, y'_{N_{R'}})$;

1: $y' = y$;
2: **for** $k' = 1$ to $N_{R'}$ **do**
3:    $y'_k = N_{Q_{k'}} + 1 - y'_k$;
4:    **if** $Fit(y') < Fit(y)$ **then**
5:       $y_k = y'_k$;
6:    **else**
7:       **if** $rand() < e^{(Fit(y')-Fit(y))}$ **then**
8:          $y_k = y'_k$;
9:       **else**
10:          $y'_k = y_k$;
11:       **end if**
12:    **end if**
13: **end for**

TABLE 1. Parameter setting.

Parameters	Value	Parameters	Value
Topology	NSFNET, CHNNET, ARPANET	Pop_{size}	100
ML	BPSK, QPSK, 8QAM, 16QAM	p_c	0.8
$d(ML)$	9600, 4800, 2400, 1200	p_m	0.2
c_{OFDM}	23.2875	p_n	0.5
d_{OFDM}	91.333	p_{n1}	0.33
c_{OXC}	100	p_{n2}	0.66
d_{OXC}	185	T	10
d_{EDFA}	30	E_{lite}	15
C_{fs}	12.5		
$c(v_i)$	15-25		

a position that the gene on this position will be changed. To generate a new gene and make the new individual be a feasible solution, step 8 to step 15 search an proper value in the candidate physical nodes.

D. LOCAL SEARCH OPERATOR

To accelerate the convergence and enhance the searching ability, a local search operator for follower variable is designed. Opposite-based search strategy and univariate search technique are used to search a better individual. In addition, if the quality of the new individual is not better than its parent individual, the new individual is accepted with a certain probability. The pseudo-code of local search operator is shown in Algorithm 4. Step 3 is exchange the gene value based opposite search strategy. Step 4 to Step 11 are to accept the new individual with a certain probability.

V. EXPERIMENTS AND ANALYSIS

To evaluate the effectiveness and efficiency of the proposed bi-level mathematical model and algorithm, a large nnumber of simulation experiments are conducted on three networks topographies. Some parameters used in the simulation experiments will be given in section V-A. In section V-B, we present the experimental results. Finally, experimental results obtained are analyzed in section V-C.

A. PARAMETERS SETTING

Each virtual node in VONs has between $2-4$ candidate nodes in EONs. Required capacity of all virtual connection requests satisfy uniform distribution in [12.5, 125], and virtual connection request exists between each pair of virtual nodes. Parameters of Physical Network and Genetic algorithm are shown in Table 1.

B. EXPERIMENTAL RESULTS

In the established bi-level mathematical model, there are leader's objective and follower's objective. Ratio of FS utilized is also an important metric for routing and spectrum assignment (RSA) algorithm. So, three metrics are used to evaluate the effectiveness of the proposed algorithm, including maximum index of used frequency slots (MIUFS), energy consumption (EC), ratio of frequency slots utilization (RFSU) defined by

$$RFSU = \frac{FS_{total}}{NL_{used} \times N(F)} \tag{20}$$

where FS_{total} and NL_{used} are the used FSs number and links number, respectively.

We compare the proposed algorithm GAL with three best performance algorithms, which solve the VONs mapping problem, denoted by CAN-A, LCSD and GRC-SVNE, respectively. CAN-A, LCSD and GRC-SVNE denote the algorithms of proposed in literature [4], literature [6] and literature [50], respectively. CAN-A algorithm lies in constructing the candidate substrate node subset and the candidate substrate path subset before embedding. This reduces the mapping execution time substantially without performance loss. In addition, four types of node and link constraints
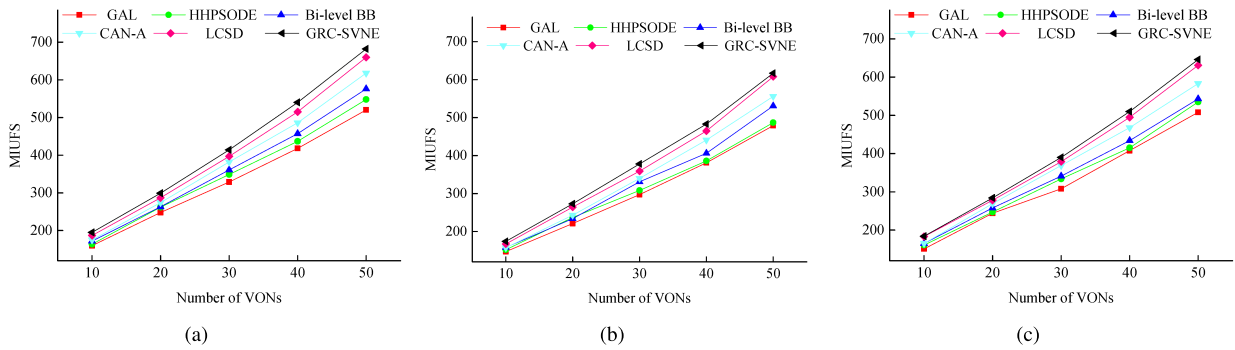
FIGURE 3. MIUFS versus number of VONs in three networks. (a) MIUFS versus number of VONs in NSFNET network; (b) MIUFS versus number of VONs in CHNNET network; (c) MIUFS versus number of VONs in ARPANET network.
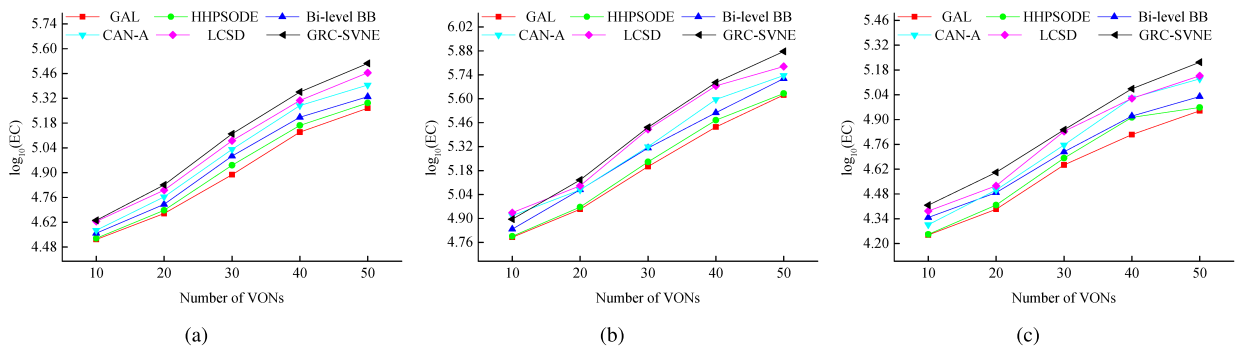

FIGURE 4. EC versus number of VONs in three networks. (a) EC versus number of VONs in NSFNET network; (b) EC versus number of VONs in CHNNET network; (c) EC versus number of VONs in ARPANET network.

are considered in the CAN-A algorithm, making it more applicable to realistic networks. To minimize the network cost for a given set of VONs, LSCD algorithm is map the largest bandwidth requirement virtual links on the shortest distance physical links. GRC-SVNE includes two phases: In node mapping phase, to improve mapping successful ratio, the mapping capacity of all nodes is calculated, and then some nodes are selected as candidate nodes for virtual network embedding. In the second phase, link mapping is performed with Dijkstra algorithm.

In addition, to demonstrate the proposed GAL can solve the bi-level optimization model effectively, two recent algorithms, which denoted by PSO and DE, are selected to compared with GAL. Literature [31] proposed a hierarchical hybrid particle swarm optimization (PSO) and differential evolution (DE) based algorithm (HHPSODE) to deal with bi-level programming problem (BLPP). A bi-level branch-and-bound ((BB) method is proposed in [12]. In bi-level BB, a spatial BB method is utilized in the higher level to solve the quadratically constrained quadratic programming (QCQP) problem, whereas a simple BB method is employed in the lower level to solve a mixed-integer quadratic programming (MIQP) problem. In the first experiment instance, we fix the number of virtual nodes with 5 in each virtual optical network, and virtual connection requests exist between each pair of virtual nodes. The number of virtual optical network

are 10, 20, 30, 40, 50. Fig.3 shows the maximum index of used frequency slots (MIUFS) obtained by the algorithms varying with number of VONs in NSFNET, CHNNET and ARPANET networks. Energy consumption (EC) of all the connection requests obtained by the algorithms varying with the number of VONs in NSFNET, CHNNET and ARPANET networks are shown in Fig.4. Fig.5 shows the ratios of frequency slots utilization (RFSU) obtained by the algorithms varying with number of VONs in NSFNET, CHNNET and ARPANET networks.

In another experiment, we fix the number of VONs as $M = 30$, but the number of virtual nodes varies from 3 to 7 in each virtual optical network. Fig.6 shows the maximum index of used frequency slots (MIUFS) obtained by the algorithms versus the number of virtual nodes in each virtual optical network on NSFNET, CHNNET and ARPANET networks. Energy consumption (EC) obtained by the algorithms versus the number of virtual nodes in each virtual optical network on NSFNET, CHNNET and ARPANET networks are shown in Fig.7. Fig.8 shows the ratios of frequency slots utilization (RFSU) obtained by the algorithms versus the number of virtual nodes in each virtual optical network on NSFNET, CHNNET and ARPANET networks.

Table 2 shows the mean and standard deviation results on the three network topologies with two instances in terms of the MIUFS. Table 3 shows the mean and standard deviation
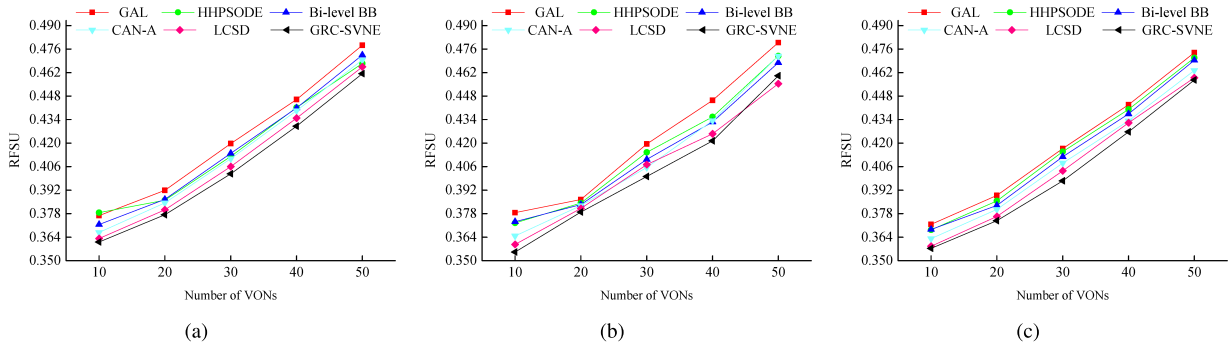
FIGURE 5. RFSU versus number of VONs in three networks. (a) RFSU versus number of VONs in NSFNET network; (b) RFSU versus number of VONs in CHNNET network; (c) RFSU versus number of VONs in ARPANET network.
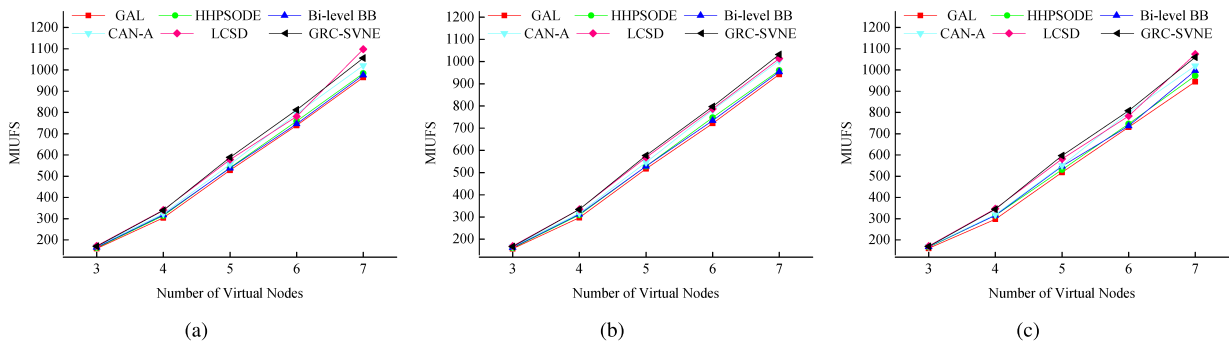

FIGURE 6. MIUFS versus the number of virtual nodes in three networks. (a) MIUFS versus the number of virtual nodes in NSFNET network; (b) MIUFS versus the number of virtual nodes in CHNNET network; (c) MIUFS versus the number of virtual nodes in ARPANET network.
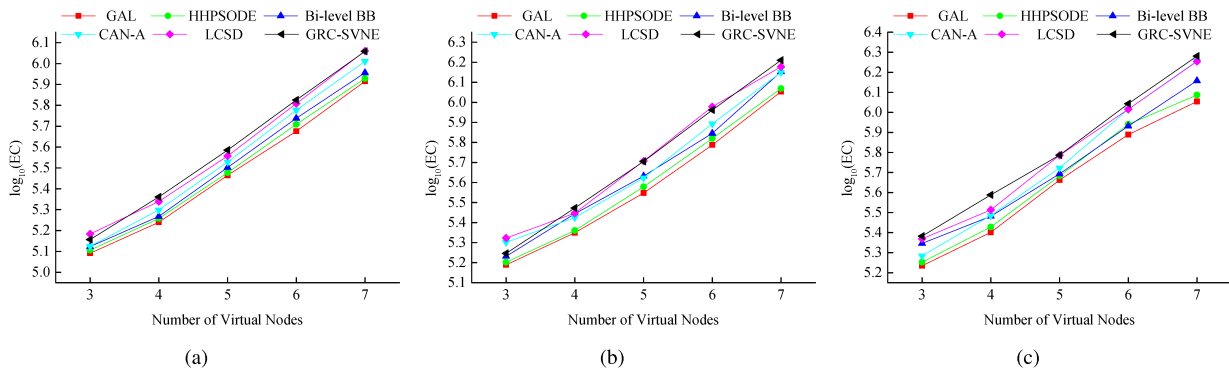

FIGURE 7. EC versus the number of virtual nodes in three networks. (a) EC versus the number of virtual nodes in NSFNET network; (b) EC versus the number of virtual nodes in CHNNET network; (c) EC versus the number of virtual nodes in ARPANET network.

results on the three network topologies with two instances in terms of the MIUFS. Table 4 shows the mean and standard deviation results on the three network topologies with two instances in terms of the MIUFS. In the three tables, the significance of difference between proposed algorithm (GAL) and the compared algorithms is determined by using the well known Wilcoxon's rank sum test [10].

C. EXPERIMENTAL ANALYSIS
In the experiments, maximum index of used frequency slots (MIUFS) obtained by the six algorithms are shown in Fig.3

and Fig.6 with two different instances. From Fig.3, we can see that the values of the maximum index of used frequency slots (MIUFS) obtained by proposed algorithm is smaller than those obtained by the compared algorithms with the number of VONs varying from 10 to 50. Similarly, the values of the maximum index of used frequency slots (MIUFS) obtained by proposed algorithm is smaller than those obtained by the compared algorithms with the number nodes in VONs from 3 to 7 as shown in Fig.6. CAN-A algorithm lies in constructing the candidate substrate node subset and the candidate substrate path subset before embedding.
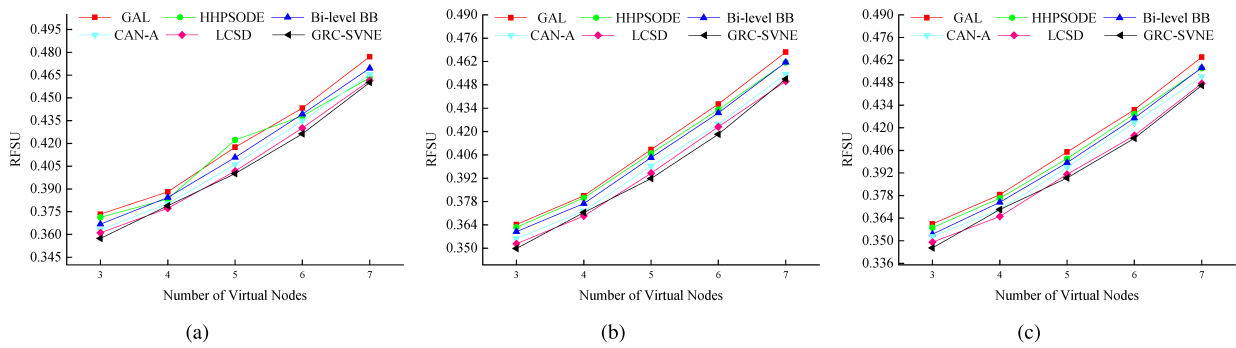
FIGURE 8. RFSU versus the number of virtual nodes in three networks. (a) RFSU versus the number of virtual nodes in NSFNET network; (b) RFSU versus the number of virtual nodes in CHNNET network; (c) RFSU versus the number of virtual nodes in ARPANET network.

TABLE 2. Statistical results (Mean and Standard Deviation) of the MIUFS.

Topology	N	M	GAL	HHPSODE	Bi-level BB	CAN-A	LCSD	GRC-SVNE
NSFNET	5	10	160 (3.55E+00)	164 (6.01E+00) +	172 (3.94E+00) +	175 (0.00E+00) +	187 (0.00E+00) +	195 (0.00E+00) +
		20	248 (6.06E+00)	262 (7.99E+00) +	263 (6.14E+00) +	274 (0.00E+00) +	287 (0.00E+00) +	299 (0.00E+00) +
		30	329 (1.10E+01)	349 (9.79E+00) +	361 (1.14E+01) +	382 (0.00E+00) +	397 (0.00E+00) +	414 (0.00E+00) +
		40	418 (1.47E+01)	437 (1.07E+01) ≈	457 (1.54E+01) +	486 (0.00E+00) +	515 (0.00E+00) +	540 (0.00E+00) +
		50	520 (2.18E+01)	548 (1.02E+01) +	576 (2.29E+01) +	618 (0.00E+00) +	660 (0.00E+00) +	682 (0.00E+00) +
	3		159 (5.94E+00)	162 (5.99E+00)≈	165 (6.39E+00) +	170 (0.00E+00) +	172 (0.00E+00) +	170 (0.00E+00) +
	4		304 (9.07E+00)	314 (9.63E+00) +	318 (9.26E+00) +	323 (0.00E+00) +	341 (0.00E+00) +	339 (0.00E+00) +
	5	30	528 (1.48E+01)	540 (1.51E+01) +	538 (1.51E+01) +	556 (0.00E+00) +	578 (0.00E+00) +	589 (0.00E+00) +
	6		739 (1.82E+01)	759 (1.86E+01) +	746 (1.81E+01) +	795 (0.00E+00) +	789 (0.00E+00) +	803 (0.00E+00) +
	7		965 (1.82E+01)	984 (1.86E+01) +	976 (1.87E+01) +	1021 (0.00E+00) +	1098 (0.00E+00) +	1056 (0.00E+00) +
CHNNET	5	10	147 (3.25E+00)	152 (2.89E+00) ≈	158 (3.52E+00) +	157 (0.00E+00) +	167 (0.00E+00) +	174 (0.00E+00) +
		20	221 (5.16E+00)	237 (5.61E+00) +	234 (5.49E+00) +	243 (0.00E+00) +	264 (0.00E+00) +	273 (0.00E+00) +
		30	297 (9.51E+00)	308 (9.75E+00) +	331 (1.04E+01) +	340 (0.00E+00) +	359 (0.00E+00) +	378 (0.00E+00) +
		40	381 (1.29E+01)	386 (1.30E+01) ≈	406 (1.37E+01) +	441 (0.00E+00) +	465 (0.00E+00) +	483 (0.00E+00) +
		50	479 (1.91E+01)	487 (1.96E+01) +	531 (2.13E+01) +	556 (0.00E+00) +	601 (0.00E+00) +	617 (0.00E+00) +
	3		157 (3.38E+00)	160 (3.33E+00) ≈	162 (3.38E+00) ≈	167 (0.00E+00) +	172 (0.00E+00) +	169 (0.00E+00) +
	4		297 (6.70E+00)	309 (6.93E+00) +	312 (7.31E+00) +	317 (0.00E+00) +	335 (0.00E+00) +	334 (0.00E+00) +
	5	30	517 (1.66E+01)	529 (1.70E+01) +	529 (1.69E+01) +	546 (0.00E+00) +	568 (0.00E+00) +	577 (0.00E+00) +
	6		721 (2.45E+01)	748 (2.55E+01) +	734 (2.49E+01) +	781 (0.00E+00) +	787 (0.00E+00) +	797 (0.00E+00) +
	7		942 (3.74E+01)	960 (3.80E+01) +	954 (3.79E+01) +	1004 (0.00E+00) +	1014 (0.00E+00) +	1032 (0.00E+00) +
ARPANET	5	10	151 (3.52E+00)	161 (3.66E+00) +	165 (2.19E+01) +	165 (0.00E+00) +	178 (0.00E+00) +	184 (0.00E+00) +
		20	244 (5.77E+00)	247 (5.79E+00) ≈	258 (3.31E+01) +	269 (0.00E+00) +	278 (0.00E+00) +	284 (0.00E+00) +
		30	308 (9.74E+00)	334 (1.07E+01) +	341 (4.02E+01) +	369 (0.00E+00) +	379 (0.00E+00) +	391 (0.00E+00) +
		40	408 (1.37E+01)	415 (1.41E+01) +	434 (4.35E+01) +	468 (0.00E+00) +	495 (0.00E+00) +	510 (0.00E+00) +
		50	508 (2.01E+01)	535 (2.12E+01) +	543 (5.63E+01) +	583 (0.00E+00) +	631 (0.00E+00) +	646 (0.00E+00) +
	3		160 (3.63E+00)	166 (1.78E+01) +	168 (1.35E+01) +	169 (0.00E+00) +	171 (0.00E+00) +	168 (0.00E+00) +
	4		297 (6.70E+00)	308 (3.36E+01) +	315(2.29E+01) +	321 (0.00E+00) +	347 (0.00E+00) +	334 (0.00E+00) +
	5	30	518 (1.66E+01)	531 (6.16E+01) +	547 (3.90E+01) +	550 (0.00E+00) +	581 (0.00E+00) +	597 (0.00E+00) +
	6		731 (2.47E+01)	746 (8.86E+01) +	737 (6.79E+01) +	800 (0.00E+00) +	783 (0.00E+00) +	808 (0.00E+00) +
	7		945 (3.74E+01)	973 (1.32E+02) +	997 (7.94E+01) +	1020 (0.00E+00) +	1075 (0.00E+00) +	1060 (0.00E+00) +
$+/-/\approx$				24/0/6	29/0/1	30/0/0	30/0/0	30/0/0

'+' indicates that GAL significantly improves the peer algorithm at a 0.05 level by Wilconxon's rank sum test. '−' indicates that peer algorithms significant improvements over GAL. If no significant difference is detected, it will be marked by the symbol '≈'. They have the same meaning in other tables.

In GRC-SVNE, link mapping is performed with Dijkstra algorithm. That will make connection requests imbalance on different links. This algorithm will obtain a lager maximum index of used frequency slots. LCSD algorithm maps the virtual nodes of the largest computing resource requirements to physical nodes of the largest available computing resources one by one, thus making connection requests imbalance on different links. However, proposed algorithm can search the optimal virtual nodes mapping scheme for all the virtual nodes and optimal routing scheme for all the connection requests using a genetic algorithm with uniform design and tailor-made genetic operators. In the first experimental instance, as shown in Fig.3, the values of the maximum index of used frequency slots obtained by the proposed algorithm are 3.5%−8.7% less than those obtained by the compared algorithms when the number of virtual optical network is 10. When the number of virtual optical network is 50, the values of the maximum index of used frequency slots obtained by the proposed algorithm are 5.1%−12.4% less than those obtained by the compared algorithms, respectively.

TABLE 3. Statistical results (Mean and Standard Deviation) of the EC.

Topology	N	M	GAL	HHPSODE	Bi-level BB	CAN-A	LCSD	GRC-SVNE
NSFNET	5	10	4.5224 (1.83E-02)	4.5290 (6.24E-01) +	4.5583 (3.74E-01) +	4.5750 (0.00E+00) +	4.6247 (0.00E+00) +	4.6304 (0.00E+00) +
		20	4.6689 (1.88E-02)	4.6873 (6.32E-01) +	4.7208 (4.40E-01) +	4.7632 (0.00E+00) +	4.8014 (0.00E+00) +	4.8308 (0.00E+00) +
		30	4.8886 (2.15E-02)	4.9418 (5.29E-01) +	4.9940 (5.25E-01) +	5.0317 (0.00E+00) +	5.0805 (0.00E+00) +	5.1186 (0.00E+00) +
		40	5.1287 (2.29E-02)	5.1669 (6.50E-01) +	5.2126 (5.35E-01) +	5.2783 (0.00E+00) +	5.3076 (0.00E+00) +	5.3551 (0.00E+00) +
		50	5.2639 (3.49E-02)	5.2938 (6.57E-01) +	5.3288 (5.51E-01) +	5.3947 (0.00E+00) +	5.4637 (0.00E+00) +	5.5167 (0.00E+00) +
	3	30	5.0913 (2.15E-02)	5.1057 (4.61E-01) +	5.1231 (5.21E-01) +	5.1245 (0.00E+00) +	5.1836 (0.00E+00) +	5.1567 (0.00E+00) +
	4		5.2392 (2.04E-02)	5.2577 (4.03E-01) +	5.2680 (5.20E-01) +	5.2988 (0.00E+00) +	5.3392 (0.00E+00) +	5.3607 (0.00E+00) +
	5		5.4645 (2.36E-02)	5.4776 (4.99E-01) +	5.5021 (5.10E-01) +	5.5279 (0.00E+00) +	5.5570 (0.00E+00) +	5.5854 (0.00E+00) +
	6		5.6759 (2.81E-02)	5.7086 (4.72E-01) +	5.7380 (5.32E-01) +	5.7767 (0.00E+00) +	5.8082 (0.00E+00) +	5.8251 (0.00E+00) +
	7		5.9149 (4.39E-02)	5.9287 (5.86E-01) +	5.9562 (5.40E-01) +	6.0108 (0.00E+00) +	6.0603 (0.00E+00) +	6.0581 (0.00E+00) +
CHNNET	5	10	4.7899 (2.02E-02)	4.7957 (2.03E-02) ≈	4.8374 (2.05E-02) +	4.9163 (0.00E+00) +	4.9341 (0.00E+00) +	4.8959 (0.00E+00) +
		20	4.9538 (1.93E-02)	4.9663 (1.94E-02) ≈	5.0676 (1.98E-02) ≈	5.0670 (0.00E+00) +	5.0907 (0.00E+00) +	5.1252 (0.00E+00) +
		30	5.2035 (2.25E-02)	5.2305 (2.26E-02) +	5.3116 (2.29E-02) +	5.3196 (0.00E+00) +	5.4212 (0.00E+00) +	5.4328 (0.00E+00) +
		40	5.4344 (2.69E-02)	5.4746 (2.71E-02) +	5.5186 (2.73E-02) +	5.5958 (0.00E+00) +	5.6750 (0.00E+00) +	5.6951 (0.00E+00) +
		50	5.6223 (4.17E-02)	5.6311 (4.18E-02) +	5.7183 (4.24E-02) +	5.7355 (0.00E+00) +	5.7884 (0.00E+00) +	5.8762 (0.00E+00) +
	3	30	5.1888 (2.10E-02)	5.2022 (5.17E-01) +	5.2318 (2.12E-02) +	5.3018 (0.00E+00) +	5.3230 (0.00E+00) +	5.2461 (0.00E+00) +
	4		5.3494 (2.15E-02)	5.3603 (5.10E-01) +	5.4443 (2.19E-02) +	5.4248 (0.00E+00) +	5.4473 (0.00E+00) +	5.4729 (0.00E+00) +
	5		5.5479 (2.44E-02)	5.5785 (4.90E-01) +	5.6320 (2.48E-02) +	5.6231 (0.00E+00) +	5.7074 (0.00E+00) +	5.7048 (0.00E+00) +
	6		5.7872 (2.58E-02)	5.8202 (5.98E-01) +	5.8453 (2.60E-02) +	5.8932 (0.00E+00) +	5.9779 (0.00E+00) +	5.9619 (0.00E+00) +
	7		6.0535 (4.02E-02)	6.0693 (6.23E-01) +	6.1533 (4.09E-02) +	6.1501 (0.00E+00) +	6.1781 (0.00E+00) +	6.2105 (0.00E+00) +
ARPANET	5	10	4.2479 (1.72E-02)	4.2512 (1.72E-02) ≈	4.3467 (4.10E-02) +	4.3057 (0.00E+00) +	4.3837 (0.00E+00) +	4.4163 (0.00E+00) +
		20	4.3931 (1.77E-02)	4.4172 (1.78E-02) +	4.4872 (5.14E-02) +	4.5020 (0.00E+00) +	4.5257 (0.00E+00) +	4.6014 (0.00E+00) +
		30	4.6437 (2.05E-02)	4.6824 (2.06E-02) ≈	4.7180 (4.70E-02) ≈	4.7561 (0.00E+00) +	4.8327 (0.00E+00) +	4.8422 (0.00E+00) +
		40	4.8147 (2.14E-02)	4.9117 (2.19E-02) +	4.9192 (4.65E-02) +	5.0215 (0.00E+00) +	5.0192 (0.00E+00) +	5.0737 (0.00E+00) +
		50	4.9491 (3.29E-02)	4.9683 (3.30E-02) ≈	5.0300 (4.81E-02) +	5.1298 (0.00E+00) +	5.1469 (0.00E+00) +	5.2229 (0.00E+00) +
	3	30	5.2343 (2.21E-02)	5.2521 (9.34E-02) +	5.3464 (2.94E-02) +	5.2840 (0.00E+00) +	5.3688 (0.00E+00) +	5.3824 (0.00E+00) +
	4		5.4012 (2.11E-02)	5.4279 (8.49E-02) +	5.4814 (2.17E-02) ≈	5.4852 (0.00E+00) +	5.5131 (0.00E+00) +	5.5886 (0.00E+00) +
	5		5.6625 (2.44E-02)	5.6831 (9.17E-02) +	5.6932 (3.24E-02) +	5.7226 (0.00E+00) +	5.7861 (0.00E+00) +	5.7865 (0.00E+00) +
	6		5.8892 (2.92E-02)	5.9404 (8.89E-02) +	5.9315 (3.83E-02) +	6.0156 (0.00E+00) +	6.0153 (0.00E+00) +	6.0432 (0.00E+00) +
	7		6.0544 (4.49E-02)	6.0865 (1.00E-01) +	6.1583 (4.83E-02) +	6.2566 (0.00E+00) +	6.2543 (0.00E+00) +	6.2807 (0.00E+00) +
$+/-/\approx$				25/0/5	26/0/4	30/0/0	30/0/0	30/0/0

Furthermore, we can see that proposed algorithm can save more frequency slots with the increase of the number of VONs. In the second experimental instance, as shown in Fig.6, the values of the maximum index of used frequency slots obtained by the proposed algorithm are 3.4%−7.6% less than those obtained by the compared algorithms when the number of virtual nodes is 3. When the number of virtual nodes is 7, the values of the maximum index of used frequency slots obtained by the proposed algorithm are 4.8%−9.6% less than those obtained by the compared algorithms, respectively. Similarly, we can see that proposed algorithm can save more frequency slots with the increase of the number of virtual nodes in each virtual optical network.

Energy consumption (EC) of all the connection requests obtained by the six algorithms is evaluated. From Fig.4 and Fig.7, we can see that energy consumption obtained by the proposed algorithm is less than that obtained by the compared algorithms. The proposed algorithm can determine an optimal virtual node mapping and routing scheme which minimizes energy consumption. In addition, modulation level selection can decrease energy consumption to the utmost extent. So, energy consumption by proposed algorithm is the smallest among all compared algorithms. As shown in Fig.4, the energy consumption by the proposed algorithm is 4.6%−10.1% less than that by the compared algorithms

when the number of virtual optical network is 10. When the number of virtual optical network is 50, the energy consumption by the proposed algorithm is 7.2%−14.8% less than that by compared algorithms, respectively. As shown in Fig.7, the energy consumption by the proposed algorithm is 5.6%−10.9% less than that by the algorithms CAN-A, GRC-SVNE and LSCD when the number of nodes in each virtual optical network is 3. When the number of nodes in each virtual optical network is 7, the energy consumption by the proposed algorithm is 7.4%−13.5% less than that by compared algorithms, respectively.

As shown in Fig.5 and Fig.8, ratios of frequency slots utilization obtained by the six algorithms are compared in three networks. The proposed algorithm using evolutionary policy make the connection requests much more balance to K candidate paths. Therefore, the proposed algorithm can obtain a higher ratio of frequency slots utilization than the five compared algorithms. As shown in Fig.5, ratios of frequency slots utilization obtained by the proposed algorithm are range of 35.8% to 48.6%, 35.4% to 48.7% and 36.1% to 49.1% with the number of VONs varying from 10 to 50 in three networks. In Fig.8, ratios of frequency slots utilization obtained by the proposed algorithm are range of 36.2% to 49.3%, 35.9% to 49.1% and 36.0% to 48.8% with the number of nodes in each virtual optical network varying from 3 to 7 in three networks. This results indicate that the proposed algorithm can increase

TABLE 4. Statistical results (Mean and Standard Deviation) of the RFSU.

Topology	N	M	GAL	HHPSODE	Bi-level BB	CAN-A	LCSD	GRC-SVNE
NSFNET	5	10	0.3768 (7.69E-03)	0.3734 (2.02E-02) +	0.3715 (1.97E-02) +	0.3668 (0.00E+00) +	0.3632 (0.00E+00) +	0.3611 (0.00E+00) +
		20	0.3919 (1.15E-02)	0.3881 (1.82E-02) +	0.3865 (1.81E-02) +	0.3844 (0.00E+00) +	0.3803 (0.00E+00) +	0.3773 (0.00E+00) +
		30	0.4197 (1.72E-02)	0.4175 (2.35E-02) ≈	0.4139 (2.38E-02) +	0.4107 (0.00E+00) +	0.4060 (0.00E+00) +	0.4017 (0.00E+00) +
		40	0.4460 (2.59E-02)	0.4433 (3.29E-02) +	0.4409 (3.26E-02) +	0.4393 (0.00E+00) +	0.4349 (0.00E+00) +	0.4301 (0.00E+00) +
		50	0.4783 (3.04E-02)	0.4770 (3.13E-02) +	0.4725 (3.14E-02) +	0.4695 (0.00E+00) +	0.4654 (0.00E+00) +	0.4614 (0.00E+00) +
	3		0.3734 (8.54E-03)	0.3713 (2.00E-02) +	0.3668 (1.11E-02) +	0.3632 (0.00E+00) +	0.3611 (0.00E+00) +	0.3574 (0.00E+00) +
	4		0.3881 (1.31E-02)	0.3834 (2.27E-02) ≈	0.3844 (1.31E-02) ≈	0.3803 (0.00E+00) +	0.3773 (0.00E+00) +	0.3789 (0.00E+00) +
	5	30	0.4175 (1.74E-02)	0.4222 (2.41E-02) −	0.4107 (1.82E-02) ≈	0.4061 (0.00E+00) +	0.4017 (0.00E+00) +	0.4001 (0.00E+00) +
	6		0.4433 (1.78E-02)	0.4380 (3.06E-02) ≈	0.4393 (1.93E-02) +	0.4349 (0.00E+00) +	0.4301 (0.00E+00) +	0.4263 (0.00E+00) +
	7		0.4771 (2.81E-02)	0.4633 (3.36E-02) +	0.4695 (2.92E-02) +	0.4654 (0.00E+00) +	0.4614 (0.00E+00) +	0.4601 (0.00E+00) +
CHNNET	5	10	0.3786 (1.42E-02)	0.3725 (1.64E-02) +	0.3732 (2.01E-02) +	0.3647 (0.00E+00) +	0.3597 (0.00E+00) +	0.3551 (0.00E+00) +
		20	0.3864 (1.84E-02)	0.3843 (1.71E-02) ≈	0.3834 (2.21E-02) ≈	0.3828 (0.00E+00) +	0.3811 (0.00E+00) +	0.3789 (0.00E+00) +
		30	0.4195 (2.35E-02)	0.4145 (2.20E-02) ≈	0.4103 (1.93E-02) ≈	0.4055 (0.00E+00) +	0.4072 (0.00E+00) +	0.4001 (0.00E+00) +
		40	0.4455 (2.54E-02)	0.4356 (2.89E-02) +	0.4326 (3.31E-02) +	0.4334 (0.00E+00) +	0.4255 (0.00E+00) +	0.4213 (0.00E+00) +
		50	0.4799 (3.37E-02)	0.4719 (2.86E-02) ≈	0.4679 (3.11E-02) ≈	0.4719 (0.00E+00) +	0.4554 (0.00E+00) +	0.4601 (0.00E+00) +
	3		0.3643 (1.50E-02)	0.3626 (1.73E-02) +	0.3601 (2.03E-02) +	0.3558 (0.00E+00) +	0.3527 (0.00E+00) +	0.3499 (0.00E+00) +
	4		0.3815 (1.74E-02)	0.3802 (1.86E-02) +	0.3768 (3.13E-02) +	0.3724 (0.00E+00) +	0.3693 (0.00E+00) +	0.3714 (0.00E+00) +
	5	30	0.4092 (1.82E-02)	0.4069 (2.52E-02) +	0.4044 (2.65E-02) +	0.3993 (0.00E+00) +	0.3950 (0.00E+00) +	0.3918 (0.00E+00) +
	6		0.4365 (2.24E-02)	0.4331 (2.52E-02) +	0.4312 (3.28E-02) +	0.4244 (0.00E+00) +	0.4228 (0.00E+00) +	0.4184 (0.00E+00) +
	7		0.4677 (3.35E-02)	0.4614 (3.66E-02) +	0.4615 (3.78E-02) +	0.4544 (0.00E+00) +	0.4501 (0.00E+00) +	0.4515 (0.00E+00) +
ARPANET	5	10	0.3716 (1.17E-02)	0.3683 (1.83E-02) +	0.3686 (1.95E-02) ≈	0.3631 (0.00E+00) +	0.3586 (0.00E+00) +	0.3573 (0.00E+00) +
		20	0.3889 (1.12E-02)	0.3856 (1.78E-02) +	0.3829 (2.09E-02) +	0.3805 (0.00E+00) +	0.3763 (0.00E+00) +	0.3738 (0.00E+00) +
		30	0.4168 (1.76E-02)	0.4149 (2.00E-02) +	0.4119 (2.47E-02) +	0.4081 (0.00E+00) +	0.4035 (0.00E+00) +	0.3975 (0.00E+00) +
		40	0.4429 (2.82E-02)	0.4401 (3.35E-02) +	0.4374 (3.21E-02) +	0.4333 (0.00E+00) +	0.4321 (0.00E+00) +	0.4267 (0.00E+00) +
		50	0.4739 (2.92E-02)	0.4708 (3.47E-02) ≈	0.4694 (2.98E-02) +	0.4633 (0.00E+00) +	0.4589 (0.00E+00) +	0.4576 (0.00E+00) +
	3		0.3604 (1.13E-02)	0.3581 (2.02E-02) +	0.3541 (1.96E-02) +	0.3527 (0.00E+00) +	0.3491 (0.00E+00) +	0.3455 (0.00E+00) +
	4		0.3785 (1.75E-02)	0.3764 (2.74E-02) +	0.3738 (1.87E-02) +	0.3693 (0.00E+00) +	0.3650 (0.00E+00) +	0.3693 (0.00E+00) +
	5	30	0.4050 (1.86E-02)	0.4008 (2.86E-02) +	0.3984 (2.30E-02) +	0.3954 (0.00E+00) +	0.3912 (0.00E+00) +	0.3889 (0.00E+00) +
	6		0.4312 (1.91E-02)	0.4285 (2.67E-02) +	0.4260 (2.04E-02) +	0.4232 (0.00E+00) +	0.4152 (0.00E+000) +	0.4135 (0.00E+000) +
	7		0.4638 (2.94E-02)	0.4569 (3.44E-02) +	0.4573 (3.33E-02) +	0.4518 (0.00E+00) +	0.4475 (0.00E+00) +	0.4462 (0.00E+00) +
+/ − / ≈				22/1/7	24/0/6	30/0/0	30/0/0	30/0/0

ratio of frequency slots utilization compared to the compared algorithms.

Table 2, Table 3 and Table 4 show the statistical results (mean and standard deviation) on the three network topologies with two instances. From the results, we can see that GAL is significant better than the five compared algorithms. CAN-A, GRC-SVNE and LSCD can not find the global optimal solution for the problem, and GAL can converge to the global optimal solution, so GAL can obtain the better solution (statistical results of mean) than that of CAN-A, GRC-SVNE and LSCD obtained. However, GAL is a randomized algorithm, the statistical results of standard deviation of GAL obtained are larger than that of CAN-A, GRC-SVNE and LSCD obtained. Uniform design and local search are used in GAL, so GAL can obtain the better solution than that of HHPSODE and bi-level BB obtained. In addition, the significance of difference between proposed algorithm (GAL) and the compared algorithms is determined by using the well known Wilcoxon's rank sum test. From the results, we can see that GAL significantly better than the compared algorithms.

D. ALGORITHM COMPLEXITY

In proposed algorithm, K shortest paths should be calculated for each connection request in advance, its complexity is $O(KN^2)$, where N is the number of nodes in a network. There are $N_{R'}$ connection requests, so the complexity for all connection requests for calculating K shortest paths is $O(KN^2 N_{R'})$. The fitness function calculation in the proposed algorithm remains the most complicated and its complexity is $O(2G_{max}Pop_{size}N^2 N_F)$, where G_{max}, Pop_{size}, and N_F denote iteration times, population size, and MIUFS. Therefore, the complexity of proposed algorithm is $O(KN^2 N_{R'} + 2G_{max}Pop_{size}N^2 N_F)$.

VI. CONCLUSION

We investigate the VONs mapping problem in EONs. A bi-level mathematical model, which minimize EC and MIUFS, is established to solve this challenging problem. In the bi-level mathematical model, leader's objective is to minimize EC, which is used to determine the optimal virtual nodes mapping scheme for all the virtual nodes and optimal routing scheme for connection requests. To minimize the MIUFS, follower's decision maker determine an optimal scheme of routing and spectrum assignment for all the connection requests. In order to solve the bi-level mathematical model effectively, we adopt uniform design method and propose a genetic algorithm with two populations. Finally, a large number of simulation experiments are conducted, and three widely used metrics are to evaluate the performance of the proposed algorithm in three widely used networks. Experimental results show that the bi-level mathematical model established is reasonable, and the proposed algorithm

are more efficient. However, the proposed algorithm has high complexity, so it is only suitable for static (off-line) VONs problem. So, some other efficient algorithms should be designed to solve the dynamic (on-line) VONs mapping problem.

REFERENCES

[1] J. F. Bard, "Some properties of the bilevel programming problem," *J. Optim. Theory Appl.*, vol. 68, no. 2, pp. 371–378, Feb. 1991.

[2] A. Cai, J. Guo, R. Lin, G. Shen, and M. Zukerman, "Multicast routing and distance-adaptive spectrum allocation in elastic optical networks with shared protection," *J. Lightw. Technol.*, vol. 34, no. 17, pp. 4076–4088, Sep. 1, 2016.

[3] H. Cao, H. Zhu, and L. Yang, "Dynamic embedding and scheduling of service function chains for future SDN/NFV-enabled networks," *IEEE Access*, vol. 7, pp. 39721–39730, 2019.

[4] H. Cao, Y. Zhu, G. Zheng, and L. Yang, "A novel optimal mapping algorithm with less computational complexity for virtual network embedding," *IEEE Trans. Netw. Service Manag.*, vol. 15, no. 1, pp. 356–371, Mar. 2018.

[5] B. Chen, W. Xie, J. Zhang, J. P. Jue, Y. Zhao, S. Huang, and W. Gu, "Energy and spectrum efficiency with multi-flow transponders and elastic regenerators in survivable flexible bandwidth virtual optical networks," in *Proc. Opt. Fiber Commun. Conf.*, 2014, pp. 1–3, paper W2A–27.

[6] B. Chen, J. Zhang, W. Xie, J. P. Jue, Y. Zhao, and G. Shen, "Cost-effective survivable virtual optical network mapping in flexible bandwidth optical networks," *J. Lightw. Technol.*, vol. 34, no. 10, pp. 2398–2412, May 15, 2016.

[7] M. Chowdhury, M. R. Rahman, and R. Boutaba, "ViNEYard: Virtual network embedding algorithms with coordinated node and link mapping," *IEEE/ACM Trans. Netw.*, vol. 20, no. 1, pp. 206–219, Feb. 2012.

[8] K. Christodoulopoulos, I. Tomkos, and E. A. Varvarigos, "Elastic bandwidth allocation in flexible OFDM-based optical networks," *J. Lightw. Technol.*, vol. 29, no. 9, pp. 1354–1366, May 1, 2011.

[9] C. Dai and X. Lei, "A multiobjective brain storm optimization algorithm based on decomposition," *Complexity*, vol. 2019, pp. 1–11, Jan. 2019.

[10] J. Derrac, S. García, D. Molina, and F. Herrera, "A practical tutorial on the use of nonparametric statistical tests as a methodology for comparing evolutionary and swarm intelligence algorithms," *Swarm Evol. Comput.*, vol. 1, no. 1, pp. 3–18, Mar. 2011.

[11] H. Ding, P. Yi, and B. Ramamurthy, "Cost-optimized reservation and routing for scheduled traffic in optical networks," *J. Opt. Commun. Netw.*, vol. 5, no. 11, pp. 1215–1226, 2013.

[12] T. Ding, R. Bo, F. Li, and H. Sun, "A bi-level branch and bound method for economic dispatch with disjoint prohibited zones considering network losses," *IEEE Trans. Power Syst.*, vol. 30, no. 6, pp. 2841–2855, Nov. 2015.

[13] Z. Ding, Z. Xu, X. Zeng, T. Ma, and F. Yang, "Hybrid routing and spectrum assignment algorithms based on distance-adaptation combined coevolution and heuristics in elastic optical networks," *Proc. SPIE*, vol. 53, no. 4, 2014, Art. no. 046105.

[14] E. Archambault, N. Alloune, M. Furdek, Z. Xu, C. Tremblay, A. Muhammad, J. Chen, L. Wosinska, P. Littlewood, and M. P. Belanger, "Routing and spectrum assignment in elastic filterless optical networks," *IEEE/ACM Trans. Netw.*, vol. 24, no. 6, pp. 3578–3592, Dec. 2016.

[15] V. Eramo and F. G. Lavacca, "Optimizing the cloud resources, bandwidth and deployment costs in multi-providers network function virtualization environment," *IEEE Access*, vol. 7, pp. 46898–46916, 2019.

[16] S. Franke, P. Mehlitz, and M. Pilecka, "Optimality conditions for the simple convex bilevel programming problem in Banach spaces," *Optimization*, vol. 67, no. 4, pp. 1–32, 2017.

[17] Z. Gao, H. Zhang, and H. Sun, "Bi-level programming models, approaches and applications in urban transportation network design problems," *J. Transp. Syst. Eng. Inf. Technol.*, vol. 4, no. 1, pp. 35–44, 2004.

[18] L. Gong and Z. Zhu, "Virtual optical network embedding (VONE) over elastic optical networks," *J. Lightw. Technol.*, vol. 32, no. 3, pp. 450–460, Feb. 1, 2014.

[19] B. Guo, C. Qiao, J. Wang, H. Yu, Y. Zuo, J. Li, Z. Chen, and Y. He, "Survivable virtual network design and embedding to survive a facility node failure," *J. Lightw. Technol.*, vol. 32, no. 3, pp. 483–493, Feb. 1, 2014. [Online]. Available: http://jlt.osa.org/abstract.cfm?URI=jlt-32-3-483

[20] J. H. Holland, *Adaptation in Natural and Artificial Systems*. Cambridge, MA, USA: MIT Press, Apr. 1975.

[21] L. Jia, Y. Wang, and L. Fan, "Multiobjective bilevel optimization for production-distribution planning problems using hybrid genetic algorithm," *Integr. Comput.-Aided Eng.*, vol. 21, no. 1, pp. 77–90, Jan. 2014.

[22] M. Jinno, B. Kozicki, H. Takara, A. Watanabe, Y. Sone, T. Tanaka, and A. Hirano, "Distance-adaptive spectrum resource allocation in spectrum-sliced elastic optical path network," *IEEE Commun. Mag.*, vol. 48, no. 8, pp. 138–145, Aug. 2010.

[23] A. Khan, A. Zugenmaier, D. Jurca, and W. Kellerer, "Network virtualization: A hypervisor for the Internet?" *IEEE Commun. Mag.*, vol. 50, no. 1, pp. 136–143, Jan. 2012.

[24] M. Kociecki and H. Adeli, "Shape optimization of free-form steel space-frame roof structures with complex geometries using evolutionary computing," *Eng. Appl. Artif. Intell.*, vol. 38, pp. 168–182, Feb. 2015.

[25] R. J. Kuo and Y. S. Han, "A hybrid of genetic algorithm and particle swarm optimization for solving bi-level linear programming problem—A case study on supply chain model," *Appl. Math. Model.*, vol. 35, no. 8, pp. 3905–3917, Aug. 2011.

[26] R. J. Kuo and C. C. Huang, "Application of particle swarm optimization algorithm for solving bi-level linear programming problem," *Comput. Math. Appl.*, vol. 58, no. 4, pp. 678–685, Aug. 2009.

[27] Y. Wang and Y.-W. Leung, "Multiobjective programming using uniform design and genetic algorithm," *IEEE Trans. Syst., Man, Cybern. C, Appl. Rev.*, vol. 30, no. 3, pp. 293–304, Aug. 2000.

[28] C. Li and L. Guo, "A single-level reformulation of mixed integer bilevel programming problems," *Oper. Res. Lett.*, vol. 45, no. 1, pp. 1–5, Jan. 2017.

[29] H. Li, L. Wang, X. Wen, Z. Lu, and J. Li, "MSV: An algorithm for coordinated resource allocation in network function virtualization," *IEEE Access*, vol. 6, pp. 76876–76888, 2018.

[30] R. Lu and X. Nan, "Survivable multipath routing and spectrum allocation in OFDM-based flexible optical networks," *J. Opt. Commun. Netw.*, vol. 5, no. 3, pp. 172–182, Mar. 2013.

[31] W. Ma, M. Wang, and X. Zhu, "Hybrid particle swarm optimization and differential evolution algorithm for bi-level programming problem and its application to pricing and lot-sizing decisions," *J. Intell. Manuf.*, vol. 26, no. 3, pp. 471–483, Jun. 2015.

[32] M. Jinno, "Virtualization in optical networks: From elastic networking level to sliceable equipment level," in *Proc. 10th Int. Conf. Optical Internet (COIN)*, May 2012, pp. 61–62.

[33] S. Peng, N. Reza, and D. Simeonidou, "Impairment-aware optical network virtualization in single-line-rate and mixed-line-rate WDM networks," *J. Opt. Commun. Netw.*, vol. 5, no. 4, pp. 283–293, 2013.

[34] P. Pongchairerks, "A two-level metaheuristic algorithm for the job-shop scheduling problem," *Complexity*, vol. 2019, pp. 1–11, Mar. 2019.

[35] M. R. Rahman and R. Boutaba, "SVNE: Survivable virtual network embedding algorithms for network virtualization," *IEEE Trans. Netw. Service Manag.*, vol. 10, no. 2, pp. 105–118, Jun. 2013.

[36] H. V. Stackelberg and A. T. Peacock, "The theory of the market economy," *Economica*, vol. 20, no. 80, p. 384, 1952.

[37] Y. Sun and J. Shen, "An energy aware routing and spectrum assignment algorithm for elastic optical network," *Study Opt. Commun.*, vol. 187, no. 1, pp. 11–13, 2015.

[38] Y.-Y. Tan, Y.-C. Jiao, H. Li, and X.-K. Wang, "MOEA/D+ uniform design: A new version of MOEA/D for optimization problems with many objectives," *Comput. Oper. Res.*, vol. 40, no. 6, pp. 1648–1660, Jun. 2013.

[39] J. L. Vizcaino, Y. Ye, V. Lopez, F. Jimenez, R. Duque, and P. M. Krummrich, "Cost evaluation for flexible-grid optical networks," in *Proc. IEEE Globecom Workshops*, Dec. 2012, pp. 358–363.

[40] C. Wang and T. Wolf, "Virtual network mapping with traffic matrices," in *Proc. 7th ACM/IEEE Symp. Archit. Netw. Commun. Syst. (ANCS)*, Oct. 2011, pp. 225–226.

[41] L. Wang, Z. Lu, X. Wen, R. Knopp, and R. Gupta, "Joint optimization of service function chaining and resource allocation in network function virtualization," *IEEE Access*, vol. 4, pp. 8084–8094, 2016.

[42] H. Xuan, Y. Wang, Z. Xu, S. Hao, and X. Wang, "Virtual optical network mapping and core allocation in elastic optical networks using multi-core fibers," *Opt. Commun.*, vol. 402, pp. 26–35, Nov. 2017.

[43] H. Xuan, S. Wei, Y. Li, and H. Guo, "Off-line time aware scheduling of bag-of-tasks on heterogeneous distributed system," *IEEE Access*, vol. 7, pp. 104777–104788, 2019.

[44] H. Xuan, S. Wei, W. Tong, D. Liu, and C. Qi, "Fault-tolerant scheduling algorithm with re-allocation for divisible task," *IEEE Access*, vol. 6, pp. 73147–73157, 2018.

[45] Y. Marinakis and M. Marinaki, "A bilevel genetic algorithm for a real life location routing problem," *Int. J. Logistics Res. Appl.*, vol. 11, no. 1, pp. 49–65, Feb. 2008.

[46] Z. Ye, A. N. Patel, P. N. Ji, and C. Qiao, "Survivable virtual infrastructure mapping with dedicated protection in transport software-defined networks," *J. Opt. Commun. Netw.*, vol. 7, no. 2, pp. A183–A189, 2015.

[47] N. Yorino, M. Abdillah, Y. Sasaki, and Y. Zoka, "Robust power system security assessment under uncertainties using bi-level optimization," *IEEE Trans. Power Syst.*, vol. 33, no. 1, pp. 352–362, Jan. 2018.

[48] Z. Zhang, W. Hu, T. Ye, W. Sun, L. Zhao, and K. Zhang, "Routing and spectrum allocation in multi-ring based data center networks," *Opt. Commun.*, vol. 360, pp. 25–34, Feb. 2016.

[49] J. Zhao, S. Subramaniam, and M. Brandt-Pearce, "Virtual topology mapping in elastic optical networks," in *Proc. IEEE Int. Conf. Commun. (ICC)*, Jun. 2013, pp. 3904–3908.

[50] X. Zheng, J. Tian, X. Xiao, X. Cui, and X. Yu, "A heuristic survivable virtual network mapping algorithm," *Soft Comput.*, vol. 23, no. 5, pp. 1453–1463, Mar. 2019.
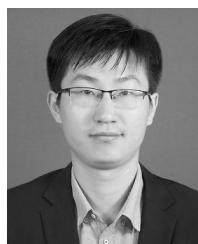
[51] Z. Zhu and B. Yu, "A modified homotopy method for solving the principal-agent bilevel programming problem," *Comput. Appl. Math.*, vol. 37, no. 1, pp. 541–566, Mar. 2018.

HEJUN XUAN received the B.Sc. degree in computer science and technology from Xinyang Normal University, China, in 2012, and the Ph.D. degree in computer software and theory from Xidian University, China, in 2018. He is currently with the School of Computer and Information Technology, Xinyang Normal University. His research interests include cloud/grid/cluster computing and scheduling in parallel and distributed systems.

SHIWEI WEI received the B.Sc. and M.Sc. degrees in computer science and technology from the Guilin University of Electronic Technology, China, in 2004 and 2007, respectively. He is currently pursuing the Ph.D. degree in computer science and technology with Xidian University, China. He is also an Assistant Professor with the Guilin University of Aerospace Technology. His research interests include cloud computing and machine learning.

YAN FENG received the Ph.D. degree in applied mathematics from Shantou University, China. He is currently a Professor with the School of Computer and Information Technology, Xinyang Normal University. His research interests include machine learning and data mining.

HUAPING GUO received the Ph.D. degree in computer science and technology from Zhengzhou University, China. He is currently an Assistant Professor with the School of Computer and Information Technology, Xinyang Normal University. His research interests include machine learning and image processing.

YANLING LI received the Ph.D. degree in computer science and technology from the Huazhong University of Science and Technology, China. He is currently a Professor with the School of Computer and Information Technology, Xinyang Normal University. His research interests include machine learning and image processing.

• • •